THE 3-D ANALYSIS OF Cu-WATER NANOFLUID INFLUENCE ON THERMAL AND HYDRAULIC PERFORMANCE IN A 30° BAFFLED COUNTERFLOW HEAT EXCHANGER

by

Hadjer BAGHNI [a]***, Imane ALIOUANE*** [a]***, Younes MENNI*** [a,b]***, Mustafa BAYRAM*** [c*]***, Omolayo M. IKUMAPAYI*** [d]***, Abiodun BAYODE*** [d]***, and Tin Tin TING*** [e,f]

[a] Department of Mechanical Engineering, Institute of Technology, University Center Salhi Ahmed Naama (Ctr. Univ. Naama),Naama, Algeria
[b] College of Technical Engineering, National University of Science and Technology, Dhi Qar, Iraq
[c] Department of Computer Engineering, Biruni University, Istanbul, Turkey
[d] Department of Mechanical Engineering, Northwest University, Potchefstroom, South Africa
[e] Faculty of Data Science and Information Technology, INTI International University, Nilai, Malaysia
[f] School of Information Technology, UNITAR International University, Selangor, Malaysia

Original scientific paper
https://doi.org/10.2298/TSCI2504131B

This study numerically analyzes a baffled counterflow heat exchanger with two adjacent side-by-side rectangular channels separated by a thin aluminum wall, allowing conductive heat transfer without fluid mixing. The hot channel carries water, while the cold Cu-water nanofluid-flows in the opposite direction. Transversal baffles, fixed in place at a 30° rotation angle, are employed to enhance thermal performance by promoting secondary flows and disrupting boundary-layers. Using the finite element method, the effects of Reynolds number (500-2000) and nanoparticle volume fraction (0%-4%) on flow structure, heat transfer, and pressure drop are investigated. Results show that increasing the nanoparticle concentration and flow rate improves thermal gradients and mixing intensity in both channels. Despite a moderate increase in pressure drop, the system achieves a maximum thermal efficiency of 35.75% under conditions of high nanoparticle concentration and low Reynolds number, confirming the effectiveness of combining nanofluids and geometric modifications for enhancing thermal performance in compact systems.

Key words: *nanofluid, counterflow, heat transfer, thermal efficiency, CFD*

Introduction

Enhancing heat exchanger performance is a key focus in thermal system design, with passive techniques such as the incorporation of internal obstacles (*e.g.*, baffles, fins, and inserts) and the use of nanofluids offering promising improvements. Baffles, particularly those featuring inclined orientations or novel geometries, have been extensively employed to generate secondary flows, disrupt thermal boundary-layers, and intensify convective heat transfer, as demonstrated by Medjahed *et al*. [1], Abidi and Sajadi [2], Tavakoli and Soufivand [3], Al-Saad *et al.* [4], Bahiraei *et al*. [5], and Ahamed *et al*. [6]. Similarly, extended surfaces such as fins and helical or curved inserts increase the effective heat transfer area and promote fluid mixing, as highlighted in the works of Rajhi *et al*. [7], Gholizadeh *et al*. [8], Jalili *et al*. [9], Wang *et al.*

* Corresponding author, e-mail: mustafabayram@biruni.edu.tr

[10], and Tahrour *et al*. [11]. Concurrently, nanofluids, engineered by dispersing nanoparticles such as Al_2O_3, Cu, or hybrid combinations into conventional base fluids, have demonstrated superior thermal conductivity and enhanced heat transport properties, particularly under laminar flow regimes, as reported by Maatki and Kriaa [12], Fereidooni [13], Bouzennada *et al*. [14], Bahiraei and Monavari [15], and Hammid *et al*. [16]. The integration of flow-altering structures with nanofluids has shown significant synergistic effects, yielding notable improvements in Nusselt number, thermal efficiency, and system compactness, as evidenced by Rajhi *et al*. [7], Bouzennada *et al*. [14], Aghaei [17], Menni *et al.* [18], and Punia and Ray [19]. In addition, recent research has increasingly focused on entropy generation and thermodynamic irreversibility as performance metrics to balance heat transfer enhancement with pressure drop penalties, as discussed by Tavakoli and Soufivand [3], Wang *et al*. [10], and Ameur *et al*. [20].

Building on previous studies, this work numerically analyzes a 3-D baffled counterflow system with two adjacent channels, one for hot water and the other for Cu-water nanofluid, separated by a conductive aluminum wall. With baffles fixed at a 30° rotation angle, the study explores the effects of Reynolds number and nanoparticle volume fraction, ϕ, on flow behavior, heat transfer, and pressure drop to enhance overall system efficiency.

Mathematical modelling and simulation strategy

The investigated system is a 3-D counterflow configuration with two adjacent rectangular channels (1 m length, 0.08 m diameter) separated by a 1 mm conductive aluminum wall enabling heat transfer without fluid mixing. Water flows as the hot fluid, while a Cu-water nanofluid (ϕ = 0%-4%) moves in the opposite direction. Transverse baffles, fixed at a 30° rotation angle, are installed on both channel walls to enhance mixing and thermal performance. The steady-state laminar flow is simulated using the finite element method, with inlet temperatures of 373.15 K (hot) and 293.15 K (cold), and Reynolds numbers ranging from 500-2000. Uniform velocity inlets, pressure outlets, adiabatic outer walls, and no-slip conditions are applied. The domain is meshed with over 1.4 million tetrahedral elements and refined near-walls and baffles for accuracy. Figure 1 shows the computational set-up. For the properties of Cu nanoparticles and water, see [21].

Flow and heat transfer are governed by the continuity, Navier-Stokes, and energy equations:

– Continuity equation

$$\frac{\partial u}{\partial x}+\frac{\partial v}{\partial y}+\frac{\partial w}{\partial z}=0 \tag{1}$$

– Momentum equations

In x-direction:

$$\rho\left(u\frac{\partial u}{\partial x}+v\frac{\partial u}{\partial y}+w\frac{\partial u}{\partial z}\right)=-\frac{\partial p}{\partial x}+\mu\left(\frac{\partial^2 u}{\partial x^2}+\frac{\partial^2 u}{\partial y^2}+\frac{\partial^2 u}{\partial z^2}\right) \tag{2a}$$

In y-direction:

$$\rho\left(u\frac{\partial v}{\partial x}+v\frac{\partial v}{\partial y}+w\frac{\partial v}{\partial z}\right)=-\frac{\partial p}{\partial y}+\mu\left(\frac{\partial^2 v}{\partial x^2}+\frac{\partial^2 v}{\partial y^2}+\frac{\partial^2 v}{\partial z^2}\right) \tag{2b}$$

In z-direction:

$$\rho\left(u\frac{\partial w}{\partial x}+v\frac{\partial w}{\partial y}+w\frac{\partial w}{\partial z}\right)=-\frac{\partial p}{\partial z}+\mu\left(\frac{\partial^2 w}{\partial x^2}+\frac{\partial^2 w}{\partial y^2}+\frac{\partial^2 w}{\partial z^2}\right) \tag{2c}$$

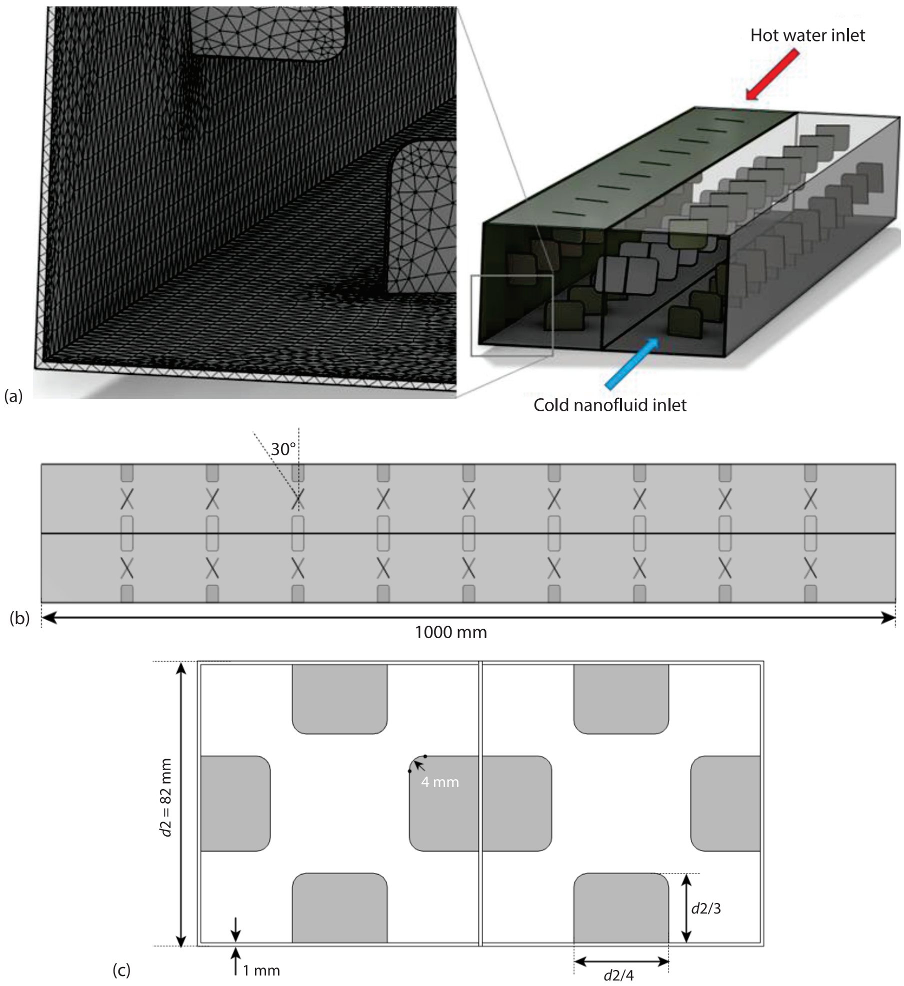

Figure 1. (a) Computational domain with mesh distribution, (b) orientation of the baffle at 30° rotation, and (c) geometric dimensions of the baffles

– Energy equation in the fluid domain

$$\rho C_p\left(u\frac{\partial T}{\partial x}+v\frac{\partial T}{\partial y}+w\frac{\partial T}{\partial z}\right)=k_f\left(\frac{\partial^2 T}{\partial x^2}+\frac{\partial^2 T}{\partial y^2}+\frac{\partial^2 T}{\partial z^2}\right) \tag{3a}$$

– Energy equation in the solid wall (Al)

$$k_s\left(\frac{\partial^2 T}{\partial x^2}+\frac{\partial^2 T}{\partial y^2}+\frac{\partial^2 T}{\partial z^2}\right)=0 \tag{3b}$$

where u, v, and w are the velocity components in the x-, y-, and z-directions, p – the pressure, ρ – the fluid density, μ – the dynamic viscosity, T – the temperature, C_p – the specific heat, and k_f and k_s are the thermal conductivity for the fluid and solid wall, respectively.

The thermophysical properties of the nanofluid are estimated by [22, 23]:

– Density, ρ_{nf}

$$\rho_{\text{nf}} = (1-\phi)\rho_{\text{bf}} + \phi\rho_{\text{np}} \tag{4a}$$

– Viscosity, μ_{nf}

$$\mu_{\text{nf}} = \frac{\mu_{\text{bf}}}{(1-\phi)^{2,5}} \tag{4b}$$

– Heat capacity, $C_{p\text{,nf}}$

$$C_{p\text{,nf}} = (1-\phi)C_{\text{p,bf}} + \phi C_{p\text{,np}} \tag{4c}$$

– Conductivity, k_{nf}

$$k_{\text{nf}} = \frac{k_{\text{np}} + 2k_{\text{bf}} + 2\phi(k_{\text{np}} - k_{\text{bf}})}{k_{\text{np}} + 2k_{\text{bf}} - \phi(k_{\text{np}} - k_{\text{bf}})} k_{\text{bf}} \tag{4d}$$

Subscripts nf, bf, and np are the nanofluid, base fluid, and nanoparticle. The thermal efficiency, η_{th}, is of the heat exchanger is defined as [24]:

$$\eta_{\text{th}} = \left(\frac{T_{c,o} - T_{c,i}}{T_{h,i} - T_{c,i}}\right) \times 100 \tag{5}$$

where $T_{c,o}$ and $T_{c,i}$ are the outlet and inlet temperatures of the cold fluid, respectively, and $T_{h,i}$ is the inlet temperature of the hot fluid. The numerical model was validated against experimental results from Laskowski [24] under identical flow and thermal conditions. As shown in tab. 1, the predicted cold fluid outlet temperatures closely match the reference data, with a maximum deviation of less than 1 °C, confirming the model's reliability.

Table 1. Cold fluid outlet temperature validation for $T_{c,i}$ = 17 °C, $\dot{m}_c$ = 0.03 kg/s, and $\dot{m}_h$ = 0.1 kg/s

$T_{h,i}$ [°C]	Present $T_{c,o}$ [°C]	$T_{c,o}$ [°C] [24]	Present ($T_{h,i} - T_{c,o}$) [°C]	($T_{h,i} - T_{c,o}$) [°C] [24]
48	24.86	25.55	23.14	22.45
49	25.11	25.85	23.89	23.15
50	25.36	26.16	24.64	23.84
51	25.61	26.47	25.39	24.53
52	25.86	26.78	26.14	25.22

Results and analysis

Figure 2 shows velocity contours in the baffled counterflow system at a 30° baffle rotation, with water as the hot fluid and 4% Cu-water nanofluid as the cold fluid, for Reynolds numbers from 500-2000. At Re = 500, flow is uniform with weak re-circulation. As Reynolds number increases, velocity gradients intensify, especially near baffles. At Re = 1500 and 2000, strong jet-like flows and re-circulation zones emerge, enhancing mixing and momentum exchange. Overall, higher Reynolds number improves secondary flows and convective transport due to the combined effects of baffles and nanofluid conductivity.

Figure 3 displays temperature contours at 30° baffle rotation and Re = 500 for varying Cu-water nanofluid volume fractions (0%-4%) in the cold channel. As ϕ increases, the cold fluid shows higher and more uniform temperatures, indicating better heat absorption. Meanwhile, the hot channel experiences a sharper temperature drop, reflecting enhanced heat transfer. The 30° baffles aid this effect by improving mixing and thermal exchange in both streams.

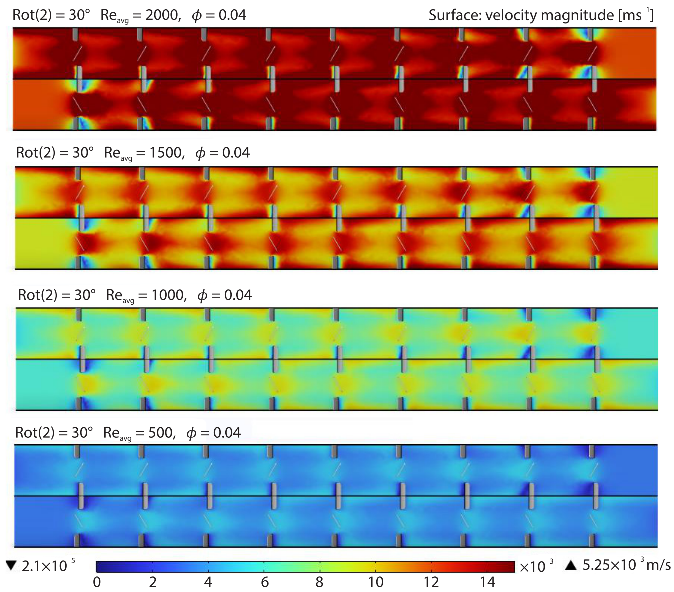

Figure 2. Velocity contours at 30° rotation for varying Reynolds number (ϕ = 0.04)

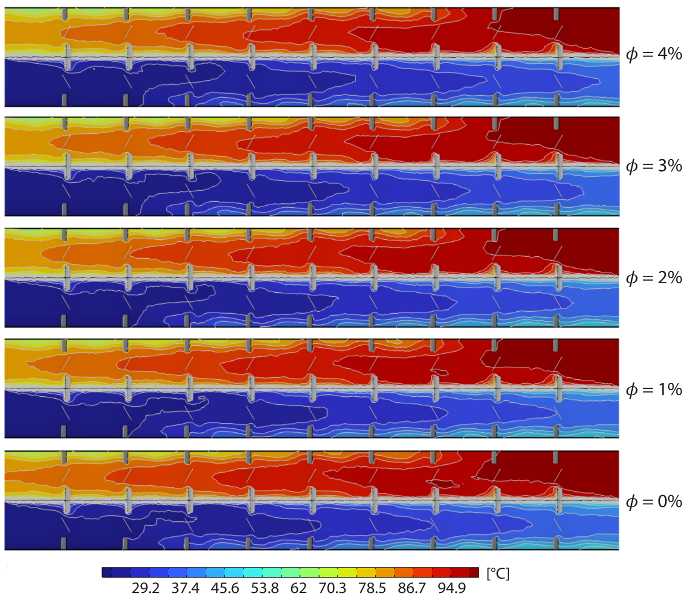

Figure 3. Temperature contours at Re = 500 for different ϕ fractions

Figure 4 shows local Nusselt number variations along the channel for different Cu-water nanofluid volume fractions (ϕ = 0%-4%) at Re = 500. The 30° baffles create periodic boundary-layer disruptions, leading to oscillating Nu profiles. Higher ϕ values consistently produce greater Nusselt number, with a peak of ~26.5 at ϕ = 0.04 *vs*. ~20.5 for ϕ = 0. Enhanced heat transfer is due to the nanofluid's thermal conductivity and baffle-induced mixing. Periodic

Nusselt number peaks reflect re-circulation and reattachment effects that thin the boundary-layer and improve wall heat transfer.

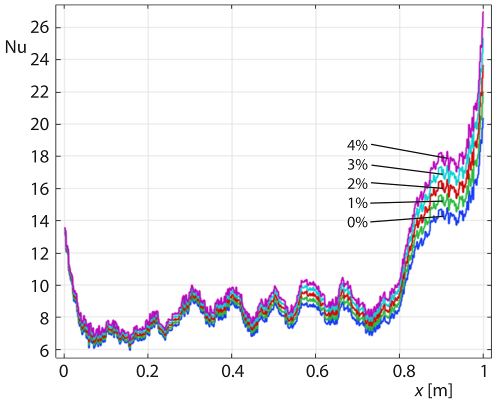

Figure 4. Local Nusselt number *vs*. *x* for varying ϕ fractions at Re = 500 (cold fluid)

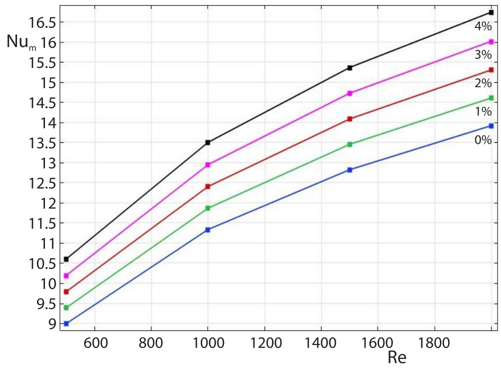

Figure 5. Average Nusselt number *vs*. Reynolds number and ϕ fraction (cold fluid)

Figure 5 shows the average Nusselt number, Nu_m, for different Reynolds numbers (500-2000) and Cu-water nanofluid volume fractions (0%-4%) at a 30° baffle rotation. The Nu_m increases with both Reynolds nymber and ϕ. For example, Nu_m rises from 8.99 (ϕ = 0%, Re = 500) to 13.92 (ϕ = 0%, Re = 2000), and from 11.34-13.51 at Re = 1000 when ϕ increases from 0%-4%. The maximum Nu_m of 16.74 occurs at ϕ = 4%, Re = 2000, an 86.2% enhancement over the base case, demonstrating strong combined effects of nanofluids and baffle-induced mixing.

Figure 6 shows the pressure drop values for the cold nanofluid under varying Reynolds numbers and nanoparticle volume fractions (ϕ = 0%-4%). At a constant nanoparticle fraction, increasing Reynolds number results in a sharp rise in pressure drop. For example, at ϕ = 0%, the pressure drop increases from 0.0381 Pa at Re = 500 to 0.5298 Pa at Re = 2000. Additionally, at a fixed Reynolds number, the pressure drop increases steadily with nanoparticle volume fraction due to the higher viscosity and density of the nanofluid. At Re = 1000, the pressure drop rises from 0.1403 Pa (ϕ = 0%) to 0.1821 Pa (ϕ = 4%), representing an approximate 30% increase. This trend is consistent across all Reynolds numbers, with slightly greater increases at higher flow rates.

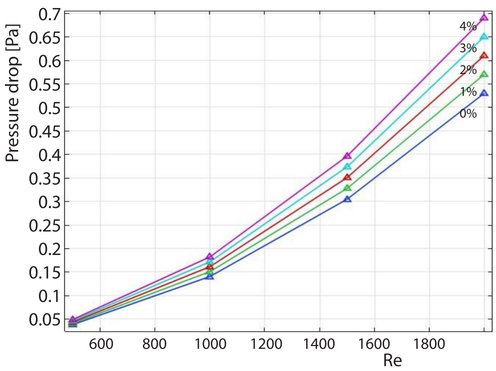

Figure 6. Pressure drop of cold nanofluid *vs*. Reynolds number and ϕ fraction

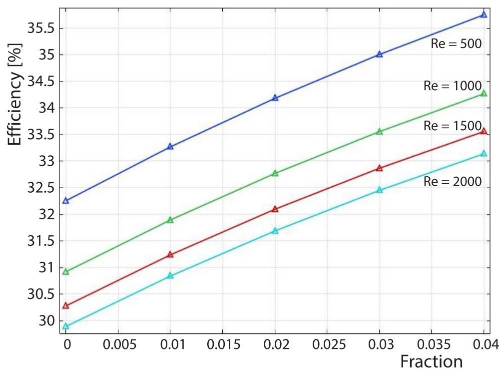

Figure 7. Thermal efficiency of the system *vs.* Reynolds number and ϕ fraction

Figure 7 presents the thermal efficiency of the baffled counterflow system using Cu-water nanofluid in the cold channel. Efficiency decreases with increasing Reynolds number due to reduced residence time, for example, from 32.25% at Re = 500 to 29.89% at Re = 2000 for pure water. In contrast, raising the nanoparticle fraction at fixed Reynolds number improves efficiency, reaching a maximum of 35.75% at $\phi = 0.04$ and Re = 500 (an 11% gain over the base case). These results highlight that combining low flow rates with nanofluids offers optimal thermal performance.

Conclusion

This study numerically analyzed a baffled counterflow system with 30° rotated baffles, using water as the hot fluid and Cu-water nanofluid as the cold fluid. The results revealed that increasing the Reynolds number from 500 to 2000 and the nanoparticle volume fraction from 0%-4% led to a substantial enhancement in heat transfer, with the average Nusselt number rising from 8.99-16.74, an improvement of over 86%. The use of nanofluids also improved thermal efficiency, with values increasing from 32.25% at $\phi = 0$-35.75% at $\phi = 0.04$ and Re = 500. However, these benefits were accompanied by a pressure drop increase of up to 30% across the same range, indicating a trade-off between thermal and hydraulic performance.

References

[1] Medjahed, *et al*. Details on the Hydrothermal Characteristics Within a Solar-Channel Heat-Exchanger Provided with Staggered t-Shaped Baffles, *Energies*, *14* (2021). 20, 6698
[2] Abidi, A., Sajadi, S. M. (2023). Numerical assessment of hydraulic behavior and thermal efficiency of multi-phase hybrid nanofluid in a shell-and-tube heat exchanger with inclined baffles. Engineering *Analysis with Boundary Elements*, *156* (2021), Nov., pp. 114-125
[3] Tavakoli, M., Soufivand, M. R., Performance Evaluation Criteria and Entropy Generation of Hybrid Nanofluid in a Shell-and-Tube Heat Exchanger with two Different Types of Cross-Sectional Baffles, *Engineering Analysis with Boundary Elements*, *150* (2023), May, pp. 272-284
[4] Al-Saad, *et al*., The Ag and Al_2O_3/Water Two-Phase Transient Flow Analysis in a Double-Pipe Heat Exchanger Equipped With Baffles And Rotating Inner Tube, *Case Studies in Chemical and Environmental Engineering*, *11* (2025), 101117
[5] Bahiraei, M., *et al*., Thermal-Hydraulic Performance of a Nanofluid pn a Shell-and-Tube Heat Exchanger Equipped with New Trapezoidal Inclined Baffles: Nanoparticle shape effect, *Powder Technology*, *395* (2022), Jan., pp. 348-359
[6] Ahamed, R., *et al.*, Thermal-Hydraulic Performance and Flow Phenomenon Evaluation of a Curved Trapezoidal Corrugated Channel with E-Shaped Baffles Implementing Hybrid Nanofluid, *Heliyon*, *10* (2024), 7, e28698
[7] Rajhi, W., *et al.*, Synergistic Effect of Outer Helical Fins and Hybrid Nanofluid on Hydrothermal Performance of Shell and Two-Coil Heat Exchanger, *Case Studies in Thermal Engineering*, *72* (2025), 106238
[8] Gholizadeh, A., *et al*., The Role of Nanofluids and Fins in a Heat Exchanger on Waste Energy Recovery from a Diesel Engine: An Experimental and Numerical Study, *Energy Reports*, *8* (2022), Nov., pp. 13353-13368
[9] Jalili, B., *et al*., Novel Usage of the Curved Rectangular Fin on the Heat Transfer of a Double-Pipe Heat Exchanger with a Nanofluid, *Case Studies in Thermal Engineering*, *35* (2022), 102086
[10] Wang, *et al.*, Two-Phase Simulation and Environmental Consideration of Thermo-Hydraulic Behavior and Entropy Production of Water/TiO_2-SWCNT Hybrid Nanofluid in a U-Shaped Heat Exchanger Equipped with Needle Fins of Different Sizes, *Engineering Analysis with Boundary Elements*, *146* (2023), 1, pp. 928-938
[11] Tahrour, *et al.*, The 3-D Numerical Study and Comparison of Thermal-Flow Performance of Various Annular Finned-Tube Designs, *Journal of Ocean Engineering and Science*, *8* (2023), 3, pp. 294-307
[12] Maatki, C., Kriaa, K., Heat Transfer Analysis for Cooling Discrete Heat Source in Micro-Channel Equipped with Flexible Baffles Using Al_2O_3-Cu/Water Hybrid Nanofluid, Case Studies in Thermal Engineering, *71* (2025), 106241
[13] Fereidooni, J., Baffles' Size Impact on the Heat Transfer and Second Law Features of Magnetic Hybrid Nanofluid Within a Hexagonal-Shaped Porous Domain, *Journal of Magnetism and Magnetic Materials*, *582* (2023), 171037

[14] Bouzennada, T., *et al*., Numerical Study on Nanofluid Heat Transfer and Fluid-Flow Within a Micro-Channel Equipped with an Elastic Baffle, *Case Studies in Thermal Engineering*, *56* (2024), 104247
[15] Bahiraei, M., Monavari, A., Irreversibility Characteristics of a Mini Shell and Tube Heat Exchanger Operating with a Nanofluid Considering Effects of Fins and Nanoparticle Shape, *Powder Technology*, *398* (2022), 117117
[16] Hammid, S., *et al*., Laminar Rarefied Flow Analysis in a Micro-Channel with H_2O-Cu Nanofluid: A Thermal lattice Boltzmann Study, *Modern Physics Letters B*, *38* (2024), 03, 2450006
[17] Aghaei, A., Thermal-Hydraulic Analysis of Syltherm 800 Thermal Oil/γ-AlOOH Nanofluid in a Baffled Shell and Tube Heat Exchanger Equipped with Corrugated Helical Tube with Two-Phase Approach, *Engineering Analysis with Boundary Elements*, *146* (2023), Jan., pp. 668-694
[18] Menni, Y., *et al*., Computational Fluid Dynamics Based Numerical Simulation of Thermal and Thermo-Hydraulic Performance of a Solar Air Heater Channel Having Various Ribs on Absorber Plates, *Mathematical Modelling of Engineering Problems*, *6* (2019), 2, pp. 170-174
[19] Punia, A., Ray, R. K., Higher-Order Super-Compact Scheme for 3-D Heat Transfer with Nanofluid and Conducting Fins, *Journal of Molecular Liquids*, *426* (2025), 127253
[20] Ameur, H., *et al*., Enhancement of the Cooling of Shear-Thinning Fluids in Channel Heat Exchangers by Using the V-Baffling Technique, *Thermal Science and Engineering Progress*, *18* (2020), 100534
[21] Hissouf, M., *et al.*, Numerical Study of a Covered Photovoltaic-Thermal Collector (PVT) Enhancement Using Nanofluids, *Solar Energy*, *199* (2020), Mar., pp. 115-127
[22] Brinkman, H. C., The Viscosity of Concentrated Suspensions and Solutions, *Journal of Chemical Physics, 20* (1952), 4, pp. 571-571
[23] Hamilton, R. L., Crosser, O. K., Thermal Conductivity of Heterogeneous Two-Component Systems, *Industrial & Engineering Chemistry Fundamentals*, *1* (1962), 3, pp. 187-191
[24] Laskowski, R., The Black Box Model of a Double-Tube Counter-Flow Heat Exchanger, *Heat and Mass Transfer*, *51* (2015), Dec., pp. 1111-1119

Paper submitted: March 2, 2025
Paper revised: May 27, 2025
Paper accepted: June 29, 2025